Adaptive Frequency Control of Microgrid Based on Fractional Order Control and a Data-Driven Control With Stability Analysis

Mohammad Verij Kazemi, Seyed Jalil Sadati, and Seyed Asghar Gholamian

***Abstract*—In this paper, a new adaptive fractional frequency control method for microgrids(MG) and low inertia networks is presented. The newly proposed grid frequency control is based on the droop and inertia controller for doubly-fed induction generator (DFIG) wind turbine (WT) using a data-driven algorithm. Also, in this paper, to ensure the grid frequency stability, the stability region boundary has been calculated using the parameter space method for above and below synchronous speeds. In the first step in the proposed method, a data-driven control (DDC) is used to update the frequency control coefficients. In the second step, in order to deployment more frequency data and to use both frequency error concavity and slope, the utilization of fractional gradient descent (FGD) and fractional inertia control is proposed. In the third step to maintain frequency stability, the updated frequency controller coefficients are compared with the stability region boundary. If the updated frequency controller coefficients are in the authorized band, they are applied. To test the proposed idea is a simulated real grid in Ontario, Canada. The simulation results indicate the proper operation of the control system in transient and steady-state and under different conditions.**

***Index Terms*—Adaptive fractional control, microgrid, data-driven control, DFIG, frequency control, stability analysis.**

I. Introduction

THE GLOBAL wind energy generation capacity is rapidly growing. Traditional WT control systems reduce the inertia of the power system due to the decoupling of mechanical rotor frequency and grid frequency. One of the generation systems that are commercially available in the wind energy market is the DFIG, which can effectively participate in power system frequency control. In [1], a multi-layer architecture method is proposed based on the foundation large-signal model that enables Microgrids (MG) to utilize in various operating points. When the weak-grid/MG frequency changes, the wind turbine (WT) can participate in frequency control. Impact and effectiveness of wind turbines in frequency control depends on electrical, mechanical parameters, and control systems of network and wind turbine. The important methods to get WT collaborating in grid frequency regulation are droop control and inertia control methods [1]–[5]. Inertia control is organized to respond to frequency droops through the usage of the kinetic energy saved in rotating masses of WTs. Variable-speed wind turbines (VSWTs) have greater kinetic power to be converted into electric energy, while the rotors speed of VSWTs is across the rated value. Therefore, using inertia control usually reduces the speed of the rotor [4]–[5]. Droop and inertia controllers are used in many control methods to improve the performance of the steady-state and transient frequency control [4], [7]–[8]. A droop control with coupling compensation and inertia control is proposed for an MG to get high dynamic performance and stability of renewable energy units [8].

In most researches, the constant gain of the frequency control loops has been considered and the effect of different values of constant gain on frequency control and power system stability has been investigated. Some recent publications focus on variable gains in the WT frequency controller [2], [4]–[5], [7]–[9]. However, they suffer from a lack of thorough analytical studies.

Recently, fractional order control (FOC) has been widely employed in several applications like load frequency control (LFC). These controllers, that their degree of freedom in designing parameters is more than the traditional controllers, improve system performance [8], [10]–[11]. Based on the authors' findings, in AC smart grids that include wind turbine and frequency control circuit installed for wind turbine and methods for updating frequency controller coefficients are provided, the stability analysis of controllers and network is not presented. In the methods that update the frequency controller coefficients, using heuristic and metaheuristic optimization algorithms, convergence, or reaching a good response depends on many parameters such as initial conditions. Additionally, in most methods of updating controller coefficients, measuring power system and WT parameters are needed, which is the accurate online measurement of these parameters. Moreover, in most of the methods presented in fractional LFC, the interchange power between areas is controlled by the FOC.

The progressively popular Gradient Descent (GD) optimization algorithms are frequently used as black

Manuscript received October 13, 2020; revised April 25, 2021 and July 21, 2021; accepted August 26, 2021. Date of publication September 9, 2021; date of current version December 23, 2021. Paper no. TSG-01455-2020. *(Corresponding author: Seyed Jalil Sadati.)*

Mohammad Verij Kazemia is with West Mazandaran Distribution Electrical Company, Nowshahr 4651674919, Iran, and also with the Faculty of Electrical and Computer Engineering, Babol Noshirvani University of Technology, Babol 4714873113, Iran (e-mail: m.v.kazemi62@gmail.com).

Seyed Jalil Sadati and Seyed Asghar Gholamian are with the Faculty of Electrical and Computer Engineering, Babol Noshirvani University of Technology, Babol 4714873113, Iran (e-mail: j.sadati@nit.ac.ir; gholamian@nit.ac.ir).

Color versions of one or more figures in this article are available at https://doi.org/10.1109/TSG.2021.3109627.

Digital Object Identifier 10.1109/TSG.2021.3109627

box optimizers when solving unrestricted problems of optimization. Each iteration of a gradient-based algorithm attempts to approach the minimizer/maximizer cost function by using the gradient's objective function information. The gradient descent technique is usually used to train by minimizing the error function, being the norm of a distance between the actual output and the desired output. Extra data compared to the traditional derivative has been accessed using fractional derivatives.

Hapsari *et al.* in [12] argued that data prediction activities entail attempts to boost predictions' accuracy by optimizing parameters in the classification algorithm. Fractional gradient descent (FGD) in support vector machine (SVM) was proposed as an unregulated optimization algorithm for objective functions in an SVM classifier. A new FGD based on a single-input interval type-2 fuzzy logic controller (SIT2-FLC) is suggested as the main LFC controller, where the footprint of uncertainty (FOU) coefficient of the SIT2-FLC is specifically adjusted to enhance the LFC performance [13].

As another important application, the complex-valued neural networks (CVNNs) are the class of networks that solve complex problems by using complex-valued variables. The GD method is one of the popular algorithms to train CVNNs. Compared with classical integer-order models, the built models in terms of fractional calculus possess significant advantages on both memory storage and hereditary characteristics. The FGD method may be analyzed for an optimal solution in a system identification problem, and a closed form Wiener solution of a least square problem is obtained. In [14], have been extended the fractional steepest descent approach to complex-valued backpropagation (CBP) neural networks training of FNNs. The batch split-complex fractional order gradient descent method for training complex value backpropagation is investigated. The monotonicity of error function and weak convergence of the proposed Caputo fractional-order CBP algorithm are derived. The standard learning algorithms of RBF neural network are based on the conventional gradient descent algorithm. Using fractional derivatives can be have access to the additional information compared to the conventional derivative that only gives a tangent at a point for the given function [15]. Fractional gradient or fractional-order calculus has been successfully used in many research applications including signal processing, control systems, bio-engineering, time series prediction, adaptive filtering, robotics, and electronics. According to the above, to study the network frequency behavior and GD method in adaptive frequency control, using the first-order derivative causes the loss of part of the frequency information.

Aiming to fill this gap, this paper proposed FOC for adaptive power system frequency control by DFIG. In this paper, the fractional-order is used in two separate cases: 1- in inertia control 2- to update the frequency controller coefficients. To use FOC, first the continued fraction approximations, and then the discretization using the Tustin method with pre-warping is done. Traditionally, the first derivative has been used in both of the above parts. The second-order derivative of frequency, on the other hand, has a lot of information about frequency. Using the second-order derivative, useful information is obtained about the trend of frequency changes. In fact, the first derivative and the second derivative show the slope and concavity, respectively. Therefore, in this paper, for better frequency control and using a wider range of frequency curve information, a fractional order derivative between 1 and 2 has been used. In the frequency controller, by combining the fractional order inertial controller and the droop controller, a more suitable active power is injected into the network to return the grid frequency to the reference value. One of the most commonly methods for updating controller coefficients is descending gradient. In this paper, for more appropriate updating of frequency controller coefficients, change of droop and inertia control coefficients based on FGD method is proposed. In particular, the Caputo derivative is utilized to fractional order gradient of the conventional quadratic energy (error) function. In this method, Jacobi vector needs to be calculated to update the controller coefficients. Due to the many advantages of using a data-driven methods, which will be discussed below, the use of these methods to calculate Jacobi vector is suggested.

The Data-Driven controller operates without the need for any information from the mathematical models of the system and it only uses the input and output data of the system. Thereupon, data-driven control (DDC) has become very popular during recent years [7]–[8], [16]–[18]. Many studies investigated the detailed modeling of WTs and power systems. However, in this paper, DDC is used to update the frequency controller coefficients without requiring measuring power system and WT parameters or power grid and the WT model. In this paper, K-Vector Nearest Neighborhood (K-VNN) approach that works well for integer-order frequency control [7] is proposed for FOC. Using the K-VNN method, the frequency is estimated for the next moment and then the frequency control coefficients are updated using the estimated frequency and FGD method.

WT operates both above and below the rated speed; there are two areas 1- limitation to rated power 2- the region of power optimization, i.e., maximum power point tracking (MPPT) [9]. To prove the stability of the power grid, the WT in both areas is modeled mathematically using a small signal model. Droop and inertia control coefficients are selected using the stability region in the parameter space method.

In view of the above, the advantages of the proposed control method can be summarized as follows:

1- It is not possible to select the constant coefficients of the frequency controller that will give an optimal response at all wind speeds and different parameters of the grid and wind turbine. Therefore, in this paper, adaptive control coefficients for the frequency control loop are proposed.
2- Since DDC requires only input and output information of the system and does not require measurement and modeling of any other system parameters, in this paper, DDC is used to update the controller coefficients.
3- The first and second derivatives of the frequency contain useful data, although none of them has all important data to power system frequency control therefore in the paper is proposed FOC in the inertia control loop.

4- A FGD is proposed to better investigate the process of frequency error changes and to find out more about the error energy function. Caputo derivative is utilized for FGD.
5- The Parameter Space method is used for obtaining the stability region boundary of the grid for above and below synchronous speeds.

Based on the authors' findings, the following points should be considered about the specific innovations of this article: 1. In no article have all the creative ideas mentioned above been combined and applied in a harmonious way. 2. Some of creative ideas mentioned above are articulated in an innovative way in our article. For example, stability analysis with adaptive fractional frequency control at above and below synchronous speed (power control mode and speed control mode) is not presented in any article.

The rest of the paper is organized as follows: Section II describes the K-VNN idea that is one of the data drive methods and Section III illustrates the Concept of FOC. Section IV is discussed the proposed method for updating the fractional frequency controller coefficients using the DDC method. In parts, Sections V and VI the stability analysis and simulation results are presented, respectively. Finally, in Section VII, the conclusion of the article is described.

II. Data-Driven Approach

Typically, to design a grid frequency control using a wind turbine, the grid and the WT should be modeled first. Although there are various and useful methods for modeling power systems and wind turbines, precise modeling is difficult and complex because precise modeling of the power systems with wind turbines is high-order, uncertain, and time-varying. Then the design and implementation of a frequency controller that performs best at all times present many challenges and difficulties. Therefore, in this paper, the use of a DDC method that operates without using the system model and only based on input and output information of the control system is used to design the network frequency controller in the wind turbine.

The data-driven approaches are divided into different classes and categories. For example, in [19] Data-driven prognostic approaches are categorized, and in [20] Different data-driven models for building energy consumption are introduced. One of the most important Data-driven algorithms is the machine learning. One of the most widely used and simple methods in machine learning is the Lazy learning (LL) method. This algorithm is very popular for many reasons, including simplicity and high speed. The main advantage gained in employing a LL method is that the target function will be approximated locally. This method is very useful for small dataset. In this article, because there is no large volume and high dimensional dataset, LL algorithms have been used.

Lazy learning, or named just-in-time learning, is rapidly developing in recent years [21], which is a memory-based modeling technique by local learning using the I/O data from the database. Specifically, the essential idea of LL is that using a query-based method to select the best model configuration at each query (i.e., the current operating point) by assessing and comparing different alternative local neighbors [22]. When the query instance is received, a set of similar related patterns is retrieved from the available training patterns set and it is used to classify the new instance. To select these similar patterns, a distance measure is used having nearby points higher relevance. LL methods generally work by selecting the k nearest input patterns to the query points, in terms of the Euclidean distance. Afterwards, the classification or prediction of the new instances is based on the selected patterns. So far, LL has been successfully applied in time series prediction, system modeling, and DDC [23].

One of the simplest and most popular LL methods is the k-nearest neighbors algorithm (K-NN). This algorithm has many advantages, the most important of which are 1- Very high speed and no need for training time 2- Very simple implementation 3- New data can be added at any time since it will affect the model. The most important drawbacks of the algorithm are: 1- not suitable for high dimensional or large dataset 2- sensitive noise and missing data 3- Feature scaling must be done. Therefore, to solve these problems and improve performance, the K-Vector Nearest Neighbor) K-VNN (algorithm, which is an extension of the K-NN algorithm, has been used. Of course, to achieve this improvement, part of the simplicity and speed of the K-VNN algorithm has been reduced. Therefore, in setting the parameters of the K-VNN algorithm, trade off must be done.

The flowchart of the K-VNN algorithm is shown in [7]. In summary, the advantages of this control method can be summarized as follows.

1- This method only requires input and output data of the frequency controller (power as output and frequency as input).
2- The distance vector is used to obtain the query point to the information data in the database. In other words, it uses both the Euclidean distance and the angle between the information to check for similarity.
3- The number of information vectors similar to the query point to estimate the current output is not known precisely In other words $k \in [k_{min}, k_{max}]$. The number of similar points to the query point estimate is increased to obtain the best estimate. Also, when the increase in the number of information vectors does not help to better estimate, the increase in the number of similar points stops.
4- This algorithm is resistant to measurement noise.
5- It is easier to implement the K-VNN algorithm than many DDC methods.
6- K-VNN prevents the addition of data and bulk of the database, and as a result, if many data is generated over time, this algorithm responds well.

III. Concept of FOC

Fractional PD controller rather than conventional PD has less sensitivity to the changes in the system parameters under control or even controller. In practical implementation, the output power of the droop controller is proportional to the

difference between the network frequency and the reference frequency of the network exactly at the same time. Also, in the frequency inertia control loop, the frequency of this moment, and the previous moment is used to calculate the frequency derivative. In addition, no other frequency information is used in the past. In other words, the concavity and convexity of a frequency curve are not important. In other words, the following two states are no different.

1- When the frequency curve is convex, and the frequency curve is descending (The first derivative of the frequency is negative, and the second derivative of the frequency is positive).
2- When the frequency curve is concave, and the frequency curve is descending (The first and second derivatives of the frequency are negative).

However, state 2 is more critical than the state 1, and the WT must use all its capacity to assist the grid frequency. Therefore, in this paper, the use of fractional order derivative (varying between state 1 and state 2) is proposed in the inertia controller to use more useful frequency information. In other words, this paper proposes the use of Eq. (1) in the frequency controller.

$$P^* = -K_{droop}\left(f_{grid} - f_{ref}\right) - K_{inertia}\left(\frac{d^r f_{grid}}{dt^r}\right) \tag{1}$$

where, P^* is the power output of the WT frequency control. f_{ref}, f_{grid}, K_{droop} and $K_{inertia}$ are the reference frequency, actual frequency, constant coefficients of droop control, and inertia, respectively and r is the fractional-order derivative.

P^* after calculation by the WT frequency controller should be generated using the direct power control (DPC) method by DFIG [24]–[25].

With a view to the implementation of fractional-order differentiators, one way is to use the estimation method that is the most vital methodology for that numerical methodology. In this methodology, Laplace operators with FOC are approximated with a transfer function with integer order. In this paper, the Oustaloup's approximation method is employed for estimation and its formulation is as follows [10]:

$$G_f(s) = K\prod_{k=1}^{N}\frac{s+\omega_k'}{s+\omega_k} \tag{2}$$

where, the poles, zeros, and gain are appraised from

$$\omega_{\mathrm{k}}' = \omega_{\mathrm{b}}\omega_{\mathrm{u}}^{(2\mathrm{k}-1-\gamma)/\mathrm{N}},\ \omega_{\mathrm{k}} = \omega_{\mathrm{b}}\omega_{\mathrm{u}}^{(2\mathrm{k}-1+\gamma)/\mathrm{N}}, \mathrm{K} = \omega_{\mathrm{h}}^{\gamma}$$

where, $\omega_{\mathrm{u}} = \sqrt{\omega_{\mathrm{h}}/\omega_{\mathrm{b}}}$. Modified Oustaloup filter is an improved filter for a FOC in the frequency range of interest $(\omega_{\mathrm{h}}, \omega_{\mathrm{b}})$.

The important step in a digital implementation of a FOC is the numerical evaluation or discretization of the fractional-order derivation s^{α}. This paper proposes discretization using the Tustin method with prewarping. The Tustin method relates to the s and z domains by using the following equation:

$$s = \frac{2}{T}\frac{z-1}{z+1} \tag{3}$$

where T is the sampling period. Finally, the discrete time fractional derivative becomes a function of z as Eq. (4).

$$s^r = F(z). \tag{4}$$

IV. Fractional Order in Adaptive Coefficients Frequency Controllers

This paper has been applied to the fractional steepest descent method to the adaptive frequency controller coefficient. In particular, the Caputo derivative is used to evaluate the fractional-order gradient of the error defined as the conventional quadratic energy function with respect to the droop and inertia controller coefficient and acquire the deterministic convergence.

In this paper, a new method for updating coefficients of the frequency controllers ($\mathrm{K_{droop}}$ and $\mathrm{K_{inertia}}$) using FGD and DDC is proposed. According to the idea of the FGD algorithm:

$$x(k) = \begin{bmatrix} \mathrm{K_{droop}}(k) \\ \mathrm{K}_{inertia}(k) \end{bmatrix} \tag{5}$$

$$x(k+1) = x(k) + \gamma g(k) \tag{6}$$

$$e(k) = f_{ref}(k) - f_{grid}(k) \tag{7}$$

$$\mathrm{J(k)} = \frac{1}{2}\,\mathrm{e(k)}^2 \tag{8}$$

$$g(k) = \begin{bmatrix} \frac{\partial^r J(k)}{\partial k_{droop}^r} \\ \frac{\partial^r J(k)}{\partial k_{inertia}^r} \end{bmatrix} \tag{9}$$

where γ is the rate of learning and x(k), e(k), g(k) and J(k) are parameters that need to be updated, error, search vector, and cost (error) function in each step respectively.

The only difference between the FGD and the traditional gradient descent is the order of derivation in Eq. (9). In the traditional gradient method, the search vector is calculated using the first-order derivative of the cost (error) function. According to the discrete-time equation, in the traditional gradient method, the frequency error depends on the current step and the last step frequency. However, in the discrete-time, FGD, other than current and the last step, errors in the previous steps are also considered.

In this paper, for the calculation of FGD, the chain rule for fractional calculus according to Eq. (10) is suggested. Finally, it is suggested to implement FGD for power frequency control using the Caputo fractional derivative definition.

$$\frac{\partial f^r}{\partial^r x} = \frac{\partial f}{\partial t}.\frac{\partial t^r}{\partial^r x} \tag{10}$$

In this paper, the changes of droop and Inertia controller coefficients in each step are calculated using Eq. (10) as Eq. (11).

$$\begin{cases} \Delta K_{droop} = -\gamma\frac{\partial J^r}{\partial^r K_{droop}} = -\gamma\frac{\partial J}{\partial u}\frac{\partial u^r}{\partial^r K_{droop}} \\ \quad = -\gamma\frac{\partial J}{\partial y}\frac{\partial y}{\partial u}\frac{\partial u^r}{\partial^r K_{droop}} \\ \quad = -\gamma\frac{\partial J}{\partial y}\frac{\partial y}{\partial u}\frac{\partial u}{\partial t}\frac{\partial t^r}{\partial^r K_{droop}} = -\gamma\frac{\partial J}{\partial y}\frac{\partial y}{\partial u}\frac{\partial u}{\partial t}\frac{1}{\frac{\partial K_{droop}{}^r}{\partial^r t}} \\ \Delta K_{inertia} = -\gamma\frac{\partial J^r}{\partial^r K_{inertia}} = -\gamma\frac{\partial J}{\partial u}\frac{\partial u^r}{\partial^r K_{inertia}} \\ \quad = -\gamma\frac{\partial J}{\partial y}\frac{\partial y}{\partial u}\frac{\partial u^r}{\partial^r K_{inertia}} \\ \quad = -\gamma\frac{\partial J}{\partial y}\frac{\partial y}{\partial u}\frac{\partial u}{\partial t}\frac{\partial t^r}{\partial^r K_{inertia}} = -\gamma\frac{\partial J}{\partial y}\frac{\partial y}{\partial u}\frac{\partial u}{\partial t}\frac{1}{\frac{\partial K_{inertia}{}^r}{\partial^r t}} \end{cases} \tag{11}$$

$\frac{\partial y}{\partial u}$ that y and u are the output and input of the power frequency controller, is the Jacobean vector. In other words, the Jacobean

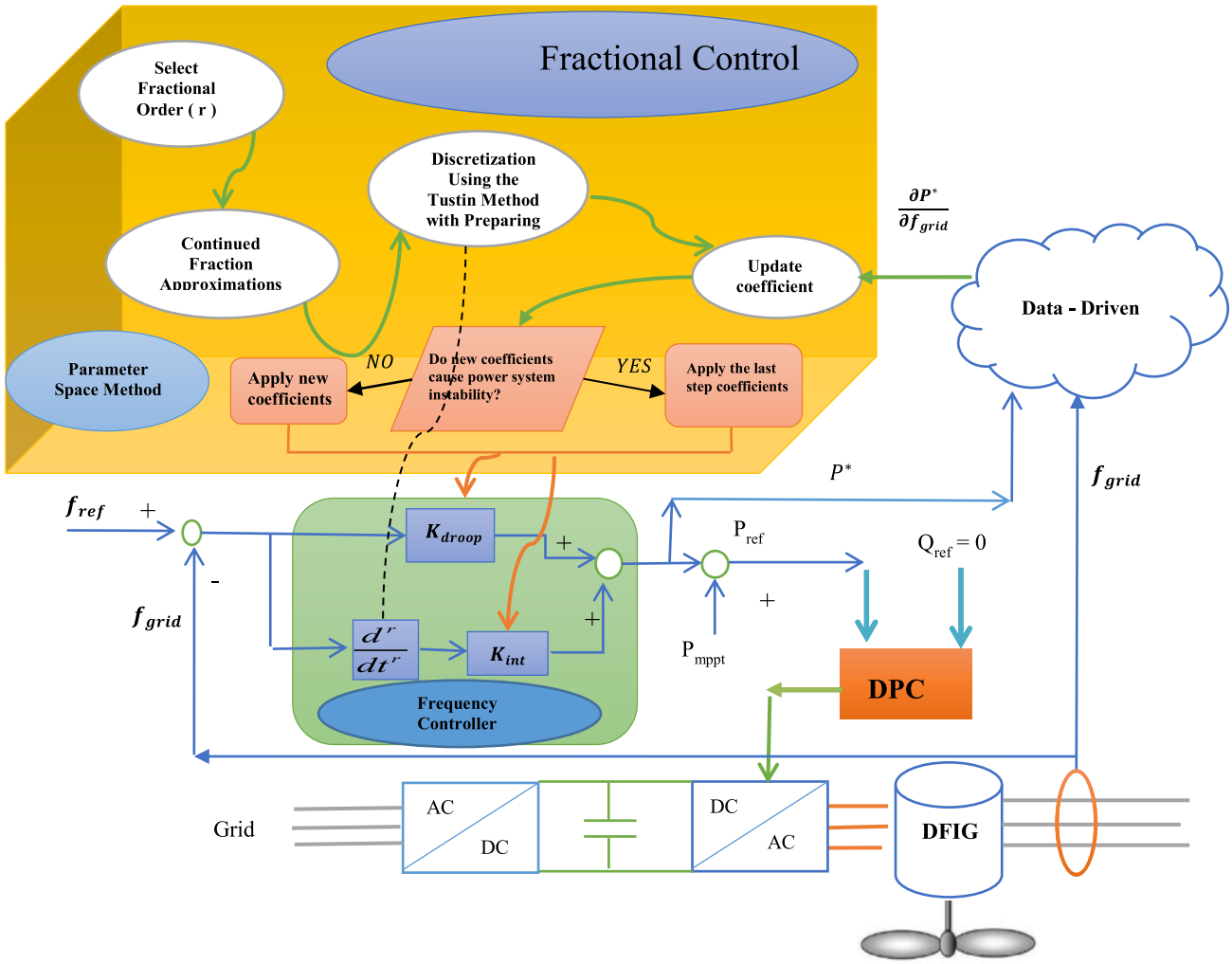

Fig. 1. Proposed method in this paper.

vector in this paper defines the changes in the output of the system relative to the changes in the input of the system, and if the system has reached a steady state, this vector becomes zero. The new idea proposed in this paper is shown in Fig. 1. As shown in Fig. 1, the input and output of the frequency controller are the grid frequency and the reference power, respectively. In this paper, DDC is used to compute the Jacobean vector $\frac{\partial P^*}{\partial f_{grid}}$. According to the above equation, updating of the droop and inertia control coefficients is proposed as Eq. (12). It can be seen in Eq. (12) that, the rate of change of frequency control coefficients depends on the Jacobean vector. This equation can be analyzed in such a way that if the grid frequency changes very little by changing the output power of the wind turbine, the changes in the frequency controller coefficients must be very large. Also, if the grid frequency changes significantly with the injection of low power by the wind turbine, there is no need to change the controller coefficients.

$$\begin{cases} \Delta K_{droop} = -\gamma e(k) \frac{\partial P^*}{\partial f_{actual}} \frac{f_{grid}(k) - f_{grid}(k-1)}{\Delta t} \frac{1}{\frac{\partial K_{droop}{}^r}{\partial r_t}} \\ \Delta K_{inertia} = -\gamma e(k) \frac{\partial P^*}{\partial f_{actual}} \frac{f_{grid}(k) - f_{grid}(k-1)}{\Delta t} \frac{1}{\frac{\partial K_{inertia}{}^r}{\partial r_t}} \end{cases} . \quad (12)$$

V. Stability Analyses

The presence of generators and consumers in the power system is always accompanied by uncertainties. Also, wind speed and frequency controller coefficients are always changing. Therefore, to ensure the robust stability of the proposed adaptive method, the stability region for different parameters variations is very important.

A. Grid and Wind Turbine Modelling

In [2], [27] a droop control implementation is presented using a small-signal model of a wind power system. In these papers, by providing stability analysis, the maximum allowable droop gain is calculated and applied to the wind turbine control system. In this paper, the equations presented in [27] are developed by considering the droop control and the inertia control simultaneously. FGD, a data-driven algorithm and stability analysis at different speeds have been used to develop the previous methods. Loads and feeders can be modeled for accurate grid modeling. Obviously, the more accurate the modeling, the more accurate the answer. Since in order to analyze the frequency stability, complete network modeling complicates the calculations and slows down the performance of the control

system, in this paper, due to references [2], [27]–[30], load and network modeling is omitted. In the future, more detailed networking will be considered.

The mechanical equation of the DFIG is as follows:

$$P_m - P_e = 2H_{DFIG}\omega_r \frac{d\omega_r}{dt} \tag{13}$$

where, P_m, P_e, H_{DFIG}, ω_r are mechanical power input of the turbine, electrical active power output, DFIG inertia constant, and rotor speed, respectively.

$$P_m = 0.5\rho c_P(\lambda,\ \beta)A_r {v_\omega}^3 \tag{14}$$

where, $\rho, c_P, \lambda, \beta, A_r, v_\omega$ are air density, power coefficient of the wind turbine, tip ratio, pitch-angle, effective area covered by the turbine blades, and wind speed.

Using small-signal modeling for Eqs. (13) and (14) the following equations have resulted:

$$\Delta P_m - \Delta P_e = 2H_{DFIG}\omega_{r0}\frac{d\Delta\omega_r}{dt} \tag{15}$$

$$\Delta P_m = A_1\Delta\beta + A_2\Delta\omega_r + A_3\Delta v_\omega \tag{16}$$

$$\begin{cases} A_1 = \frac{\partial P_m}{\partial \beta} = 0.5\ \rho\ A_r {v_\omega}^3\ \frac{\partial c_P}{\partial \beta} \\ A_2 = \frac{\partial P_m}{\partial \omega_r} = 0.5\ \rho\ A_r {v_\omega}^3\ \frac{\partial c_P}{\partial \lambda}\ \frac{\partial \lambda}{\partial \omega_r} \\ A_3 = \frac{\partial P_m}{\partial \omega_r} = 0.5\ \rho\ A_r\left(3\ c_P\ {v_\omega}^2 + {v_\omega}^3 \frac{\partial c_P}{\partial \lambda}\ \frac{\partial \lambda}{\partial v_\omega}\right) \end{cases}$$

It can be written using Eqs. (15) and (16).

$$\Delta P_e = A_1\Delta\beta + A_2\Delta\omega_r + A_3\Delta v_\omega - 2H_{DFIG}\omega_{r0}\frac{d\Delta\omega_r}{dt} \tag{17}$$

According to Eq. (1), active power injection to the grid as follows:

$$P_e = P_{normal} - K_{droop}\left(f_{grid} - f_{ref}\right) - K_{int}\left(\frac{d^r f_{grid}}{dt^r}\right) \tag{18}$$

P_{normal} is the power injected into the network under normal control conditions without frequency distortion. In most cases and typically, above and below the rated wind speed, two different control targets are implemented in the wind turbine. Below the rated wind speed, the goal is to convert the most wind energy into electrical energy. Because the parameters of the wind turbine such as rotor and stator current, electric power, speed rotation of the blades, pressure and torque applied to the blades are less than the nominal and allowable values, the parameters of the wind turbine are adjusted to achieve the MPPT. At this point, MPPT is intended to get the maximum electrical energy from wind energy, so the pitch angle is set to zero. At higher wind speeds, the continued MPPT method causes parameters of the wind turbine such as rotor speed and power and generated by wind generator to exceed their nominal values. Therefore, above the rated wind speed with pitch angle control, the rated torque (maximum torque allowed) is derived from the wind turbine. At speeds higher than the rated speed, the control goal in a wind turbine is to convert part of the wind energy into electrical energy. Therefore, the purpose of controlling these speeds is to adjust the wind turbine parameters to the nominal value. In other words, by setting these parameters to the nominal value, the maximum electrical power that the turbine is allowed to convert into electrical energy occurs. Therefore, the wind turbine model has been investigated in two different modes, above and below the rated wind speed.

1) Below the Rated Wind Speed: According to the above explanation at below the rated wind speed, P_{normal} in Eq. (18) is equal with the output power of the MPPT controller, which is represented by P_{mppt}. In the MPPT area can be written:

$$P_{mppt} = K_{opt}{\omega_r}^3 \tag{19}$$

According to Eqs. (18) and (19), the small-signal modeling for a WT, in this case, can be written as Eq. (20):

$$\Delta P_e = 3K_{opt}{\omega_r}^2\Delta\omega_r - K_{droop}\Delta f - K_{int}s^r\Delta f \tag{20}$$

where s is Laplace operator. The pitch angle in the MPPT area is zero, so based on the Eqs. (17)-(20), we will have

$$\Delta\omega_r = \frac{(K_d + K_{int}s^r)\Delta f + A_3\Delta v_\omega}{2H_{DFIG}\omega_{r0}s + 3K_{opt}{\omega_r}^2 - A_2} \tag{21}$$

By substituting Eq. (21) in Eq. (20):

$$\begin{aligned}\Delta P_e = &\left(-1 + \frac{3K_{opt}{\omega_r}^2}{2H_{DFIG}\omega_{r0}s + 3K_{opt}{\omega_r}^2 - A_2}\right)\\ &\left(K_{droop} + K_{int}s^r\right)\Delta f\\ &+ \frac{A_3 3K_{opt}{\omega_r}^2}{2H_{DFIG}\omega_{r0}s + 3K_{opt}{\omega_r}^2 - A_2}\ \Delta v_\omega.\end{aligned} \tag{22}$$

2) Above the Rated Wind Speed: Above the rated wind speed, the pitch-angle controller is used to limit the wind power output and its rotational speed. In this area, the WT torque is kept at the nominal value indicated by T_{max}. As a result, P_{normal} in Eq. (18) is equal to $P_{pow-req}$ in Eq. (23).

$$P_{pow-req} = T_{max}\omega_r \tag{23}$$

$$\Delta P_e = T_{max}\Delta\omega_r - K_{droop}\Delta f - K_{int}s^r\Delta f \tag{24}$$

This fact results in bypassing the pitch compensation block, which normally tries to reduce the output power to the rated value. Pitch angle variations are calculated as follows:

$$\Delta\beta = \frac{\left(k_{pp}s + k_{pi}\right)\Delta\omega_r}{\left(1 + \tau_p s\right)s} \tag{25}$$

where k_{pp}, k_{pi} *and* τ_p are the pitch angle PI controller variables and turbine pitch mechanical time constant, respectively. By substituting Eq. (25) in Eq. (17):

$$\begin{aligned}\Delta P_e = &A_1\frac{\left(k_{pp}s + k_{pi}\right)\Delta\omega_r}{\left(1 + \tau_p s\right)s} + A_2\Delta\omega_r + A_3\Delta v_\omega\\ &- 2H\omega_{r0}s\Delta\omega_r\end{aligned} \tag{26}$$

By equating the Eq. (18) and Eq. (26) will be:

$$\Delta\omega_r = \frac{K_{droop}\Delta f + K_{int}s^r\Delta f + A_3\Delta v_\omega}{T_{max} - \frac{(k_{pp}s+k_{pi})A_1}{(1+\tau_p s)s} - A_2 + 2H\omega_{r0}s} \tag{27}$$

By substituting Eq. (27) in Eq. (26) will be:

$$\begin{aligned}\Delta P_e = &\frac{d_2s^2 + d_1 s}{b_3s^3 + b_2s^2 + b_1 s + b_0}\Delta v_\omega\\ &+ \frac{a_3s^{r+3} + a_2s^{r+2} + a_1s^{r+1} + a_0s^r + c_3s^3 + c_2s^2 + c_1 s + c_0}{b_3s^3 + b_2s^2 + b_1 s + b_0}\Delta f\end{aligned} \tag{28}$$

Based on the single area model of load frequency control and WT modeling, the grid model considered in this paper is shown in Fig. 2. G_1 and G_2 are obtained from Eq. (22) and Eq. (28).

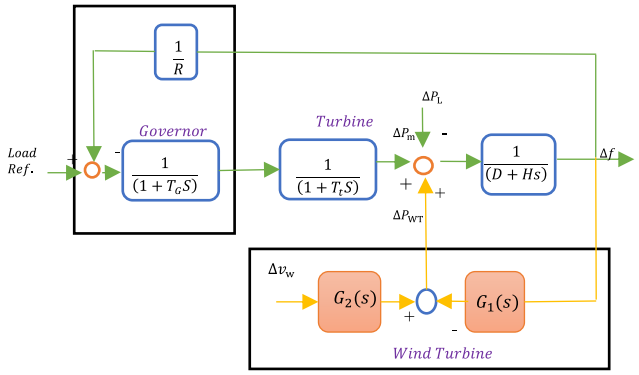

Fig. 2. Block-diagram of the single area with wind turbine model.

B. Stability Region in the Parameter Space Method

In this section, an analytical computation stability region in the parameter space method is considered to ensure the power system stability by applying the proposed frequency control method [31]–[33]. In order to obtain a stable region in the parameter space method, it is necessary to obtain the system characteristic equation presented in Fig. 2.

Only the equation G_1 affects the characteristic equation, and G_2 does not play a role in the attribute characteristic equation. According to Section V-A, two different states above and below the synchronous speed must be considered. Above and below synchronous speeds, the system characteristic equation is calculated as Eqs. (29) and (30), respectively.

$$\Delta = 1 + \frac{1}{(D+Hs)[R(1+T_GS)(1+T_tS)]} + \frac{(2H_{DFIG}\omega_{r0}s + 3K_{opt}\omega_r{}^2 - A_2 - 3K_{opt}\omega_r{}^2)(K_{droop} + K_{int}s^r)}{(D+Hs)[2H_{DFIG}\omega_{r0}s + 3K_{opt}\omega_r{}^2 - A_2]} \quad (29)$$

The stability region in the parameter space method relies on

$$\Delta = 1 + \frac{1}{(D+Hs)[R(1+T_GS)(1+T_tS)]} + \frac{a_3s^{r+3} + a_2s^{r+2} + a_1s^{r+1} + a_0s^r + c_3s^3 + c_2s^2 + c_1s + c_0}{(D+Hs)[b_3s^3 + b_2s^2 + b_1s + b_0]} \quad (30)$$

The computation of stability boundary locus by equating both the imaginary and real parts of the characteristic equation to zero.

In order to obtain the stable area and set (K_{droop}, K_{int}) of the PD^r controller, first, we substitute $s = j\omega$ then set both real and imaginary parts of the characteristic equation to zero. In this step, the equations are given as follows:

$$\begin{cases} K_d\ A_d(\omega) + K_d\ B(\omega) + C_d = 0 \\ K_{int}\ A_{int}(\omega) + K_{int}\ B_{int}(\omega) + C_{int} = 0 \end{cases} \quad (31)$$

By solving two equations in Eq. (31) simultaneously, the stability boundary locus in (K_{droop}, K_{int}) the plane is obtained. The curve on (K_{droop}, K_{int}) the plane will be obtained by drawing K_d, K_{int} based on different values of ω. The boundary locus enclosed between curves, $K_d = 0$ and $K_{int} = 0$ is a stable region.

Note that due to the system characteristic equation being different from each other sub-and super-synchronous speed, the stable regions in (K_{droop}, K_{int}) planes are different from each other sub-and super-synchronous speed, to avoid K_{droop}, K_{int} step changes when passing synchronous speeds, the common

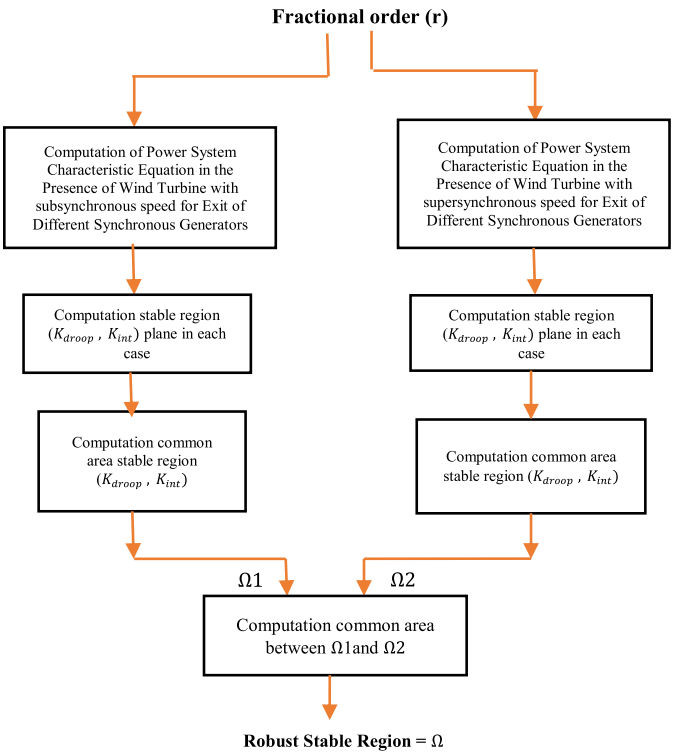

Fig. 3. Calculation robust stable region in (K_{droop}, K_{int}) plane.

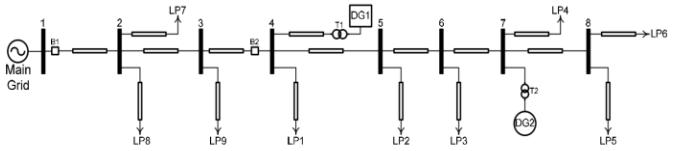

Fig. 4. The real distribution system in Ontario under study.

area stable in the plane (K_{droop}, K_{int}) at sub-and super-synchronous speed must be selected as the stable area in every fractional order.

The stability area in each fractional order is calculated offline on (K_{droop}, K_{int}) plane. The flowchart calculation of the Robust Stable Region in each fractional order is demonstrated in Fig. 4. In order to have a robust stable region, which is permanently stable for every fractional order, the intersection of all stable regions considering all possible faults is calculated. Then, one of the following steps is investigated and according to the algorithm shown in Fig. 5, the frequency control coefficients are updated.

1. After updating K_d, K_{int}, if K_{droop}, K_{int} are in the smallest stable region then apply to the control system.
2. After updating K_d, K_{int}, if K_{droop}, K_{int} are not in the smallest stable region in the current step, K_d, K_{int} must remain the same as the previous step applied to the system.

VI. Simulation Result

The time-domain simulations are used to verify the analytical results reported in the previous sections. The system studied in this section is shown in Fig. 4, which is a typical

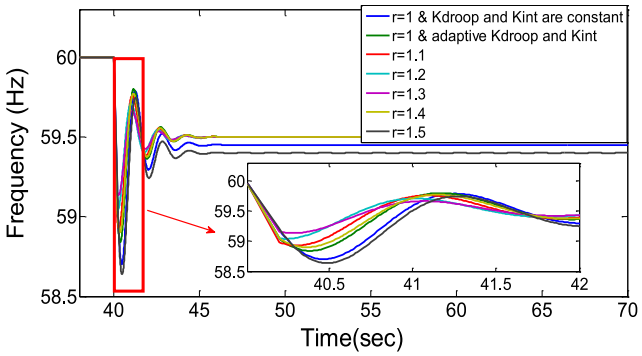

Fig. 5. Frequency grid in case 1.

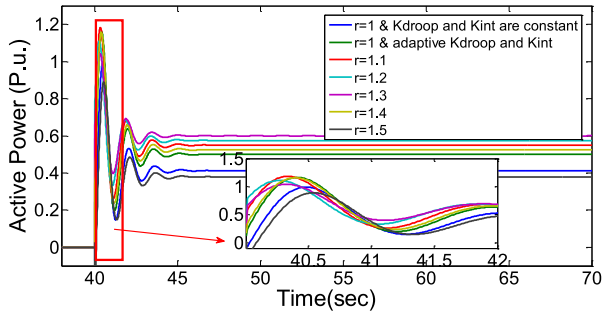

Fig. 6. Power output the frequency controller in case 1.

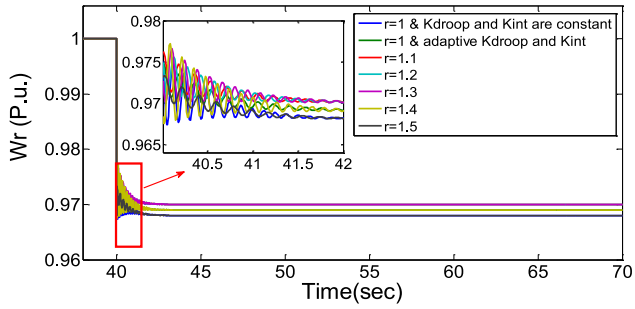

Fig. 7. Rotor speed DFIG in case 1.

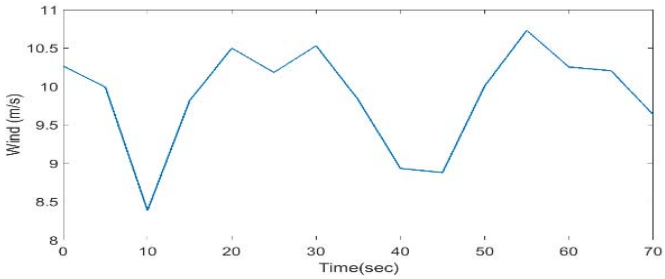

Fig. 8. Wind speed in case 2.

medium-voltage rural distribution system, a real system in Ontario, Canada. The section after the circuit breaker B2 can operate in the islanded mode and constitute an MG. It contains two DG units. DG1 is a 2.5MVA DFIG and DG2 is a 2.5 MVA synchronous generator. The rural distribution grid lines mentioned above, with a low X/R ratio (X/R = 2), are modeled as lumped R-L, as well as loads are modeled by parallel R-L circuits. Intentional islanding at t = 40s has happened as a disturbance for the distribution grid. As the disturbance occurs, the power balance between the demand and the generation is destroyed. Grid parameters and distributed generation sources are listed in [2], [24].

In order to better and more accurately survey the proposed idea, 2 different cases have been simulated in this article, and 7 different modes have been analysed and compared in each case. In the first mode, r = 1, and the coefficients of the droop and inertia controller circuit are considered constant. In the second mode, r = 1 is investigated, but the coefficients of the droop and inertia controller are updated according to the proposed algorithm. In third mode r = 1.1, fourth mode r = 1.2, fifth mode r = 1.3, sixth mode r = 1.4, seventh mode r = 1.5 is evaluated.

A. Case 1

In this case, the constant wind speed is 6m/s. The reason for choosing low speed for wind turbines in this part is that wind turbines have lower inertia energy at low speeds and it is difficult for them to participate in controlling the islanding distribution system frequency.

The MG frequency, the output power of the WT, and WT speed are shown in Figs. 5, 6, and 7, respectively. In all these Figures, to study the performance of the proposed control system in steady-state, the simulation is first displayed up to 70 seconds. Afterward, for a more precise investigation of the performance of each control method in the transient, the first 2 seconds of the feeder separation from the main network is shown.

By observing Figures 5–7, it can be seen that the grid remains stable in all control modes, but the frequency fluctuations in the traditional control mode with fixed control coefficients are high, and with increasing the degree of fractional order derivation, frequency fluctuations decrease and frequency nadir increases. As a result, by increasing the fractional-order derivation of the controller system, the WT injects more power into the network to keep the frequency constant. At this time, with the loss of kinetic energy of the wind turbine, its speed decreases more. However, with increasing derivation order higher than 1.3 the frequency fluctuations increase and frequency nadir decreases. As a result, the frequency drop in the steady-state is more and the performance of the control system becomes unsuitable. According to the studies done in this case, increasing the fractional-order derivation greater than 1.3 does not improve the efficiency of the control system. One of the most important reasons for the proper performance of the proposed control method is the proper performance of DDC and accurate frequency prediction by the KVNN algorithm. To better and more accurately studying of the above figures, some parameters are shown in Table I. r represents the fractional derivation order and the absolute value of ROCOF (Hz / s) is examined and shown in the Table I. The maximum values of ROCOF, steady state frequency, frequency error, Frequency nadir and Min (wr) is obtained for r = 1.3.

B. Case 2

For a better analysis of the proposed control method in the dynamic state, the wind speed is chosen according to Fig. 8.

TABLE I
SIMULATION RESULTS IN CASE 1

	r=1 & coefficients are constant	r=1 & coefficients are adaptive	r=1.1	r = 1.2	r = 1.3	r = 1.4	r = 1.5
Max (ROCOF(Hz/s))	0.751	0.729	0.689	0.668	0.627	0.691	0.706
Steady state frequency error(Hz)	59.488	59.498	59.499	59.501	59.502	59.499	59.408
Frequency nadir(Hz)	58.702	58.749	58.935	59.045	59.148	57.905	58.642
Min (w_r (p.u.))	0.9670	0.9689	0.9710	0.9711	0.9715	0.9674	0.9670

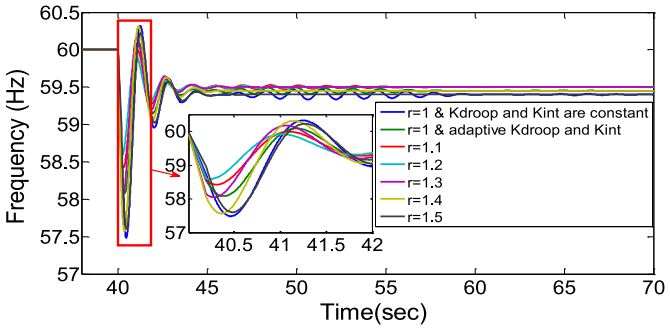

Fig. 9. Frequency grid in case 2.

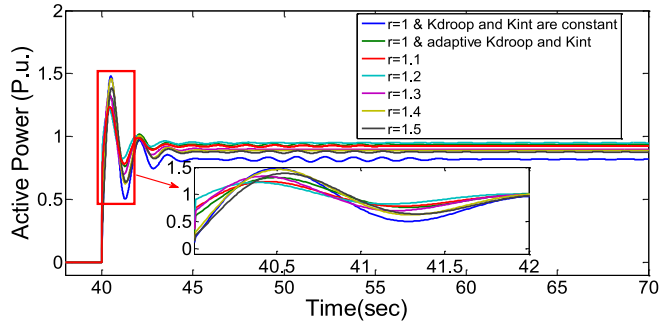

Fig. 10. Power output the frequency controller in case 2.

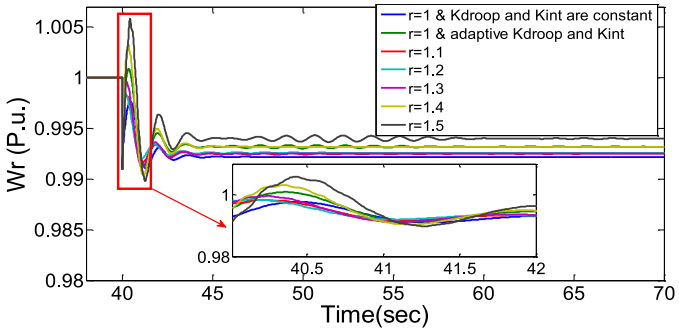

Fig. 11. Rotor speed DFIG in case 2.

In this case, as in case 1, to better evaluate the performance of the control system in transient and steady-state, islanding MG frequency, WT speed, and output power in the timescales of 40 to 42 seconds and 40 to 70 seconds are shown in Figs. 9–11.

In traditional control, the droop and inertia control coefficients are constant, the frequency fluctuates in the steady-state, which causes the WT speed and output power to fluctuate. By increasing the fractional derivation order to 1.2 in the frequency controller, the fluctuations of the distribution network frequency, WT speed, and output power decrease.

Further increase of derivation frequency intensifies the fluctuations of MG frequency, WT speed, and output power. The frequency nadir also has its maximum value for fractional derivation order 1.2 and Frequency nadir decreases with increasing or decreasing fractional-order derivation. Careful investigation of Figs. 9–11 and shows that the control system operates well even in severe wind fluctuations. Updating the controller coefficients will cause more power to be injected by the WT during turbulence, thus improving the frequency, but this improvement is achieved by reducing the rotor speed and losing the rotor kinetic energy. It should be noted that the control circuit's proper performance owes its proper frequency prediction based on past instant information using the KVNN technique.

For better and more accurate studying of the above figures, four parameters are shown in Table II. As can be observed, the maximum value of ROCOF parameters achieves for r = 1.3 and the maximum value of Min (wr) is obtained for r = 1.3 and r = 1.2. The maximum values of Steady state frequency error and Frequency nadir parameters achieve for r = 1.2.

According to grid codes, part of the capacity of a wind turbine in the event of a fault is allocated to the proper injection of reactive power and its cooperation in voltage regulation. The present paper focuses only on active power and frequency control and does not provide a method for reactive power and voltage control. When the grid frequency is equal to the reference frequency, the droop and inertia control have no output, and in fact, the proposed control idea is not sensitive to voltage changes. When voltage changes or faults occur, special control methods must be considered to inject reactive power into the network. When injecting reactive power into the network in the event of a fault, the limiters expressed in each grid code must be applied to the wind turbine frequency controller. According to the simulations, the proposed control idea has the ability to inject more active power into the network when there are frequency changes. So, if during the fault occurs, the need to inject less active power and more reactive power, the limiter should be applied according to the grid codes. Therefore, it should be noted that by implementing the proposed control method, from a practical and theoretical

TABLE II
SIMULATION RESULTS IN CASE 2

	r=1 & coefficients are constant	r=1 & coefficients are adaptive	r=1.1	r = 1.2	r = 1.3	r = 1.4	r = 1.5
Max (ROCOF(Hz/s))	0.968	0.923	0.876	0.875	0.859	0.895	0.908
Steady state frequency error(Hz)	59.390	59.401	59.489	59.512	59.519	59.451	59.445
Frequency nadir(Hz)	57.491	58.088	58.421	58.590	58.159	57.576	57.608
Min (w_r (p.u.))	0.9911	0.9913	0.9917	0.9919	0.9919	0.9903	0.9898

point of view, there is no limit in injecting the active power of the wind turbine according to the code grid when a fault occurs. The advantage of the proposed control method is when the frequency changes. If the goal is to inject reactive power due to voltage limitations, proposed control method has no advantage over other frequency control methods. To be more precise, frequency control methods are not used when the grid voltage changes [34]–[36].

C. Stability Analysis of Robust Adaptive Proposed Method

At first glance, it may seem that the higher the reference power calculated by the frequency controller, the faster the network frequency returns to the desired range (this power must eventually be generated by DFIG). Nevertheless, in practice this does not happen for a number of reasons. It can be stated with certainty; excessive increase of droop and inertia controller coefficients does not improve the frequency. The most important reasons why calculating high reference power by a frequency controller does not help to improve the frequency are described below.

1- Wind turbine because of various mechanical and electrical limitations such as wind speed, maximum torque and power, inertia, is not able to generate any power calculated by the frequency controller. At this point, there is a big difference between the reference power that the wind turbine should generate and the power that the wind turbine actually generates. In fact, the wind turbine power control circuit can not work properly (Figure 2). This can cause power and frequency fluctuations and have a negative impact on frequency stability.

2- If in a short moment the active power output of the wind turbine increases greatly (this issue may occur due to the high frequency controller coefficient), the speed of the turbine may drop sharply and enter the unauthorized range (for DFIG the allowable range is 0.7 Up to 1.3 synchronous speed). Even if the speed drops sharply and does not enter the unauthorized range, the wind turbine may no longer be able to inject the proper active power in the short term. In practice, it can be seen that the frequency improves well in a few moments, but suddenly the frequency deviates from the previous recovery path (frequency improves at a slower rate or does not improve at all).

3- If we observed the transfer of power between the grid and the wind turbine from a mechanical point of view, we find that the grid and the wind turbine each rotate with their own inertia and exchange energy with each other. In the steady state, these inertias (masses) are rotating at a synchronous speed. If too much energy is injected into the grid rotating mass through wind turbine rotating mass for short moments, power and frequency fluctuations may occur. This point depends on many parameters, including the idea and control structure, and the inertia of the turbine and network.

According to the above points, the purpose of updating the controller coefficients is appropriate adjustment and selecting large droop and inertia coefficients that do not cause improper frequency. In some articles, for such reasons, limiters such as speed, power and torque are considered. Performing several simulations in terms of network frequency stability had the same result.

If the droop and inertia controller coefficients, fixed numbers outside the stability boundaries are selected (adaptive control is not applied), then frequency instability occurs in the network. Performing more simulations by updating the frequency controller coefficients showed that if the frequency controller coefficients go out of the stability region and then enter the stability region rapidly in next update steps, frequency stability may not occur.This is a complex issue as to whether or not frequency stability occurs after the controller coefficients return to the stability region. In this case, frequency stability depends on many parameters such as electrical and mechanical parameters of the network and wind turbine, the length of time the droop and inertia coefficients were outside the stability region, the amount of coefficients outside and inside the stability region. In the control idea presented in this paper, to ensure the network frequency stability and to prevent severe mechanical stresses to the wind turbine, the frequency controller coefficients are not allowed to enter instability area. To ensure proper operation of the proposed control method, the obtained stability region boundary is considered 10% smaller.

In this part, the stability of cases 1 and 2 are analyzed. For calculation stability region boundary by using the parameter space method, the real and imaginary parts of the characteristic islanding MG equation are set to zero. After calculating the stability region boundary in the (K_{droop}, K_{int}) plan, K_{droop} and K_{int} must be in the stability region at all times to maintain the islanding microgrid frequency stability. Therefore, at each step after calculating the updated coefficients, if K_{droop} and K_{int} were the instability region,

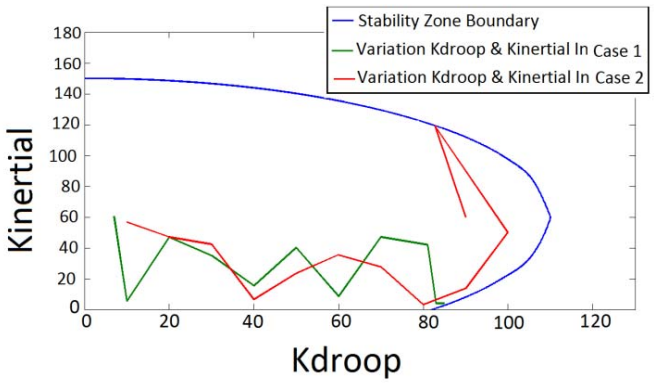

Fig. 12. Stability region of the power system in the parameter space method for r = 1.1.

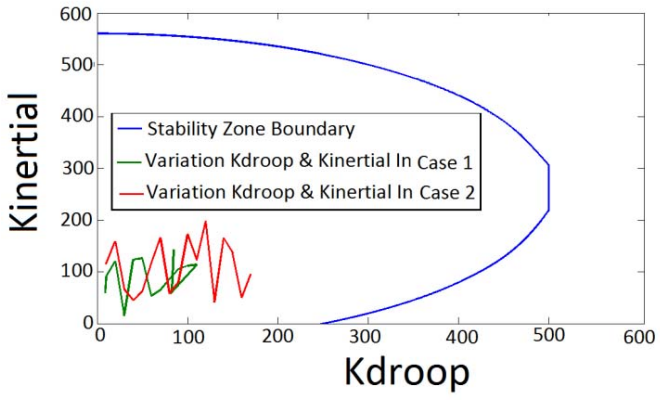

Fig. 13. Stability region of the power system in the parameter space method for r = 1.5.

K_{droop} and K_{int} would be updated in the frequency controller. If even one of the K_{droop} and K_{int} coefficients are out of stability region, both coefficients remain at their previous values and updated coefficients are not applied to the circuit.

For instance, the stability region in the (K_{droop}, K_{int}) plan and the frequency controller coefficient variations are shown in Figs. 12–13 for cases 1 - 2. It can be seen, with increasing fractional order, the stability region becomes larger. Also, the controller coefficient variations in case 2 are more than case 1. This is due to wind variations in case 2. The proposed control system in Case 2 tries to adjust the frequency control coefficients to its best value at all times, thus applying any changes to K_{droop} and K_{int}. Figure 12 shows that the droop and inertia controller coefficients are 83 and 119, respectively, when placed on the stability region boundary. In steps of updating when the frequency controller coefficients were intended to go outside the stable area, the controller did not allow exit from the stable area. The frequency controller coefficients are kept on the boundaries until the droop and inertia coefficients are selected from the stable region in future update steps. Reducing rate learning is a good way to prevent the exiting controller coefficients from the stability region during the update. However, it should be noted that selecting a very small value for rate learning causes small and inappropriate changes to the controller coefficients. In this article, 0.0005 is considered for rate learning.

VII. Conclusion

Today, frequency control of MG, islanded distribution network and weak grids are the main challenges for designers and operators. In the case of wind turbines on the network, due to the variability of wind speed and uncertainty of their production capacity, frequency control is more complex.

In this paper, a new method for adaptive frequency control in wind turbine DFIG is proposed. In the proposed method, the adaptive control of droop and inertia coefficients is based on DDC and FOC. KVNN is used to implement DDC to predict frequency. To benefit from the trend of frequency variation, FOC is used in 1- inertia controller and 2- gradient descent. Also, in this paper, to ensure the grid frequency stability, the stability region has been calculated using the parameter space method for above and below synchronous speeds. Droop and inertia control coefficients are not applied to the frequency controller after updating if they are not in the stability region.

To evaluate the performance of the proposed control system, a real grid in Ontario, Canada is simulated. By increasing the order of fractional derivative to about 1.3, the fluctuations frequency and frequency drop decrease, but the performance of the control system deteriorates as the derivative order increases further. Therefore, the best fractional-order derivative value in a wind turbine frequency controller in an isolated a real grid in Ontario is 1.3. In the simulations performed in different networks so far, the best fractional derivation order value was 1.2 or 1.3. However, with certainty, the best fractional derivation order cannot be extended to all isolated MG/weak grids before the necessary simulations. What is the best fractional derivation order in the wind turbine frequency controller depends on the electrical and mechanical parameters of the network and wind turbine. Necessary checks and simulations should be performed before setting the fractional derivation order in the frequency control circuit.

References

[1] R. Zamora and A. K. Srivastava, "Multi-layer architecture for voltage and frequency control in networked microgrids," *IEEE Trans. Smart Grid*, vol. 9, no. 3, pp. 2076–2085, May 2018.

[2] M. F. M. Arani and Y. A.-R. I. Mohamed, "Dynamic droop control for wind turbines participating in primary frequency regulation in microgrids," *IEEE Trans. Smart Grid*, vol. 9, no. 6, pp. 5742–5751, Nov. 2018.

[3] J. Zhao, X. Lyu, Y. Fu, X. Hu, and F. Li, "Coordinated microgrid frequency regulation based on dfig variable coefficient using virtual inertia and primary frequency control," *IEEE Trans. Energy Convers.*, vol. 31, no. 3, pp. 833–845, Sep. 2016.

[4] J. Lee, G. Jang, E. Muljadi, F. Blaabjerg, Z. Chen, and Y. C. Kang, "Stable short-term frequency support using adaptive gains for a DFIG-based wind power plant," *IEEE Trans. Energy Convers.*, vol. 31, no. 3, pp. 1068–1079, Sep. 2016.

[5] M. Hwang, E. Muljadi, J.-W. Park, P. Sorensen, and Y. C. Kang, "Dynamic droop–based inertial control of a doubly-fed induction generator," *IEEE Trans. Sustain. Energy*, vol. 7, no. 3, pp. 924–933, Jul. 2016.

[6] X. Meng, J. Liu, and Z. Liu, "A generalized droop control for grid-supporting inverter based on comparison between traditional droop control and virtual synchronous generator control," *IEEE Trans. Power Electron.*, vol. 34, no. 6, pp. 5416–5438, Jun. 2019.

[7] M. Verij Kazemi, S. A. Gholamian, and J. Sadati, "Adaptive frequency control with variable speed wind turbines using data-driven method," *J. Renew. Sustain. Energy*, vol. 11, no. 4, Jul. 2019, Art. no. 043305.

[8] M. V. Kazemi, S. A. Gholamian, and J. Sadati, "Adaptive fractional-order control of power system frequency in the presence of wind turbine," *IET Gener. Transm. Distrib.*, vol. 14, no. 4, pp. 594–605, Feb. 2020, doi: 10.1049/iet-gtd.2019.0458.

[9] Z. Yan and Y. Xu, "Data-driven load frequency control for stochastic power systems: A deep reinforcement learning method with continuous action search," *IEEE Trans. Power Syst.*, vol. 34, no. 2, pp. 1653–1656, Mar. 2019.

[10] S. Saxena, "Load frequency control strategy via fractional-order controller and reduced-order modeling" *Int. J. Elect. Power Energy Syst.*, vol. 104, pp. 603–614, Jan. 2019.

[11] D. Mohanty and S. Panda, "Fractional order based controller for frequency control of hybrid power system," in *Proc. IEEE Int. Conf. Sustain. Energy Technol. (ICSET)*, 2019, pp. 087–092.

[12] D. P. Hapsari, I. Utoyo, and S. W. Purnami, "Fractional gradient descent optimizer for linear classifier support vector machine," in *Proc. 3rd Int. Conf. Vocational Educ. Elect. Eng. (ICVEE)*, Surabaya, Indonesia, 2020, pp. 1–5, doi: 10.1109/ICVEE50212.2020.9243288.

[13] M. H. Khooban and M. Gheisarnejad, "A novel deep reinforcement learning controller based type-II fuzzy system: Frequency regulation in microgrids," *IEEE Trans. Emerg. Topics Comput. Intell.*, vol. 5, no. 4, pp. 689–699, Aug. 2021, doi: 10.1109/TETCI.2020.2964886.

[14] J. Wang, G. Yang, B. Zhang, Z. Sun, Y. Liu, and J. Wang, "Convergence analysis of caputo-type fractional order complex-valued neural networks" *IEEE Access*, vol. 5, pp. 14560–14571, 2017.

[15] M. Kleinz and T. Osler "A child's garden of fractional derivatives," *College Math. J.*, vol. 31, no. 2, p. 82, 2000.

[16] M.-H. Khooban, T. Niknam, M. Shasadeghi, T. Dragicevic, and F. Blaabjerg, "Load frequency control in microgrids based on a stochastic noninteger controller," *IEEE Trans. Sustain. Energy*, vol. 9, no. 2, pp. 853–861, Apr. 2018.

[17] S. Liu *et al.*, "Data-driven condition monitoring of data acquisition for consumers' transformers in actual distribution systems using t-statistics," *IEEE Trans. Power Del.*, vol. 34, no. 4, pp. 1578–1587, Aug. 2019.

[18] Z. Li, Z. Zheng, and R. Outbib, "Adaptive prognostic of fuel cells by implementing ensemble echo state networks in time-varying model space," *IEEE Trans. Ind. Electron.*, vol. 67, no. 1, pp. 379–389, Jan. 2020.

[19] M. Ahsan, S. Stoyanov, and C. Bailey, "Prognostics of automotive electronics with data driven approach: A review," in *Proc. 39th Int. Spring Seminar Electron. Technol. (ISSE)*, 2016, pp. 279–284, doi: 10.1109/ISSE.2016.7563205.

[20] Y. Wei *et al.*, "A review of data-driven approaches for prediction and classification of building energy consumption," *Renew. Sustain. Energy Rev.*, vol. 82, no. 1, pp. 1027–1047, 2018.

[21] Z. Hou, S. Liu, and T. Tian, "Lazy-learning-based data-driven model-free adaptive predictive control for a class of discrete-time nonlinear systems," *IEEE Trans. Neural Netw. Learn. Syst.*, vol. 28, no. 8, pp. 1914–1928, Aug. 2017, doi: 10.1109/TNNLS.2016.2561702.

[22] I. M. Galván, J. M. Valls, N. Lecomte, and P. Isasi, "A lazy approach for machine learning algorithms," in *Proc. Artif. Intell. Appl. Innov. III. AIAI*, vol. 296, 2009, pp. 517–522. [Online]. Available: https://doi.org/10.1007/978-1-4419-0221-4_60

[23] F. Liu and Y. Deng, "A fast algorithm for network forecasting time series," *IEEE Access*, vol. 7, pp. 102554–102560, 2019, doi: 10.1109/ACCESS.2019.2926986.

[24] M. V. Kazemi, M. Moradi, and R. V. Kazemi, "Fuzzy logic control to improve the performance of the direct power control based DFIG," *COMPEL Int. J. Comput. Math. Elect. Electron. Eng.*, vol. 33, nos. 1–2, pp. 254–272, Dec. 2013.

[25] M. V. Kazemi, A. S. Yazdankhah, and H. M. Kojabadi, "Direct power control of DFIG based on discrete space vector modulation," *Renew. Energy*, vol. 35, no. 5, pp. 1033–1042, May 2010.

[26] H. Mahvash, S. A. Taher, M. Rahimi, and M. Shahidehpour, "DFIG performance improvement in grid connected mode by using fractional order [PI] controller," *Int. J. Elect. Power Energy Syst.*, vol. 96, pp. 398–411, Mar. 2018.

[27] M. F. M. Arani and Y. A. I. Mohamed, "Analysis and impacts of implementing droop control in DFIG-based wind turbines on microgrid/weak-grid stability," *IEEE Trans. Power Syst.*, vol. 30, no. 1, pp. 385–396, Jan. 2015.

[28] H. Bevrani, F. Habibi, P. Babahajyani, M. Watanabe, and Y. Mitani, "Intelligent frequency control in an AC microgrid: Online PSO-based fuzzy tuning approach," *IEEE Trans. Smart Grid*, vol. 3, no. 4, pp. 1935–1944, Dec. 2012, doi: 10.1109/TSG.2012.2196806.

[29] M. F. M. Arani and Y. A. I. Mohamed, "Cooperative control of wind power generator and electric vehicles for microgrid primary frequency regulation," *IEEE Trans. Smart Grid*, vol. 9, no. 6, pp. 5677–5686, Nov. 2018, doi: 10.1109/TSG.2017.2693992.

[30] P. Sahu, R. Prusty, and S. Panda, "Optimal design of a robust FO-multistage controller for frequency awareness of an islanded AC microgrid under i-SCA algorithm" *Int. J. Ambient Energy*, to be published, doi: 10.1080/01430750.2020.1758783.

[31] Ş. Sönmez and S. Ayasun, "Gain and phase margins based delay-dependent stability analysis of two-area LFC system with communication delays," in *Proc. 10th Int. Conf. Elect. Electron. Eng. (ELECO)*, 2017, pp. 1409–1413.

[32] S. Sönmez and S. Ayasun, "Stability region in the parameter space of PI controller for a single-area load frequency control system with time delay," *IEEE Trans. Power Syst.*, vol. 31, no. 1, pp. 829–830, Jan. 2016.

[33] S. J. Sadati, A. Ranjbar, and R. Ghaderi, "Stability region of Smith-predictor based fractional-order PID controller for a time-delay system," in *Proc. IFAC*, 2012.

[34] Y. Poullikkas, A. Demokritou, P. Al-Assaf, and Y. T. Pavlos, "Grid code requirements for wind power integration in Europe" in *Proc. Conf. SN*. 2013, Art. no. 437674.

[35] M. Altin, Ö. Göksu, R. Teodorescu, P. Rodriguez, B. Jensen, and L. Helle, "Overview of recent grid codes for wind power integration," in *Proc. 12th Int. Conf. Optim. Elect. Electron. Equip.*, Brasov, Romania, 2010, pp. 1152–1160, doi: 10.1109/OPTIM.2010.5510521.

[36] P. Sonkar and O. P. Rahi, "Contribution of wind power plants in grid frequency regulation: Current perspective and future challenges," *Wind Eng.*, vol. 45, no. 2, pp. 442–456, 2020.

Mohammad Verij Kazemi was born in Nowshahr, Iran, in 1983. He received the B.Sc. degree in electrical engineering from Gilan University, Gilan, Iran, in 2006, and the M.Sc. degree in electrical engineering from Sahand University of Technology, Tabriz, Iran, in 2008, and the Ph.D. degree in electrical engineering from Babol Noshirvani University of Technology, Mazandaran, Iran, in 2020. He is currently working with the University and with West Mazandaran Distribution Electrical Company. His research interests include renewable energy conversion, smart grid, data-driven, and evolutionary optimization algorithms.

Seyed Jalil Sadati was born in Behshahr, Iran, in 1979. He received the M.Sc. degree from Ferdowsi University of Mashhad in 2005, and the Ph.D. degree in control engineering from the University of Mazandaran, Iran, in 2011. From 2011, he is an Assistant Professor of Control Engineering with the Department of Electrical and Computer Engineering, Babol Noshirvani University of Technology. His research interests are fractional-order control, time delay systems, nonlinear control, adaptive systems, and model predictive control.

Seyed Asghar Gholamian was born in Babolsar, Iran, in 1976. He received the B.Sc. degree in electrical engineering from K. N. Toosi University of Technology, Tehran, Iran, in 1999, the M.Sc. degree in electric power engineering (electrical machines) from the University of Mazandaran, Babol, Iran, in 2001, and the Ph.D. degree in electrical engineering from K. N. Toosi University of Technology in 2009. He is currently an Associate Professor with the Department of Electrical Engineering, Babol Noshirvani University of Technology, Iran. His research interests include design, simulation, and modeling of electrical machines.